Electronic Supplementary Information (ESI)

Highly Efficient Synergistic CO_2 Conversion with Epoxide Using Copper Polyhedron-Based MOFs with Lewis Acid and Basic Sites

Jiaming Gu,[a] Xiaodong Sun,[b] Xinyao Liu,[a] Yang Yuan,[a] Hongyan Shan,[a] and Yunling Liu*[a]

[a] *State Key Laboratory of Inorganic Synthesis and Preparative Chemistry, College of Chemistry, Jilin University, Changchun 130012, P. R. China. Fax: +86-431-85168624; Tel: +86-431-85168614; E-mail: yunling@jlu.edu.cn.*

[b] *Institute of Clean Energy Chemistry, Key Laboratory for Green Synthesis and Preparative Chemistry of Advanced Materials, College of Chemistry, Liaoning University, Shenyang 110036, P. R. China.*

Table of Contents

S1 Supporting Figures

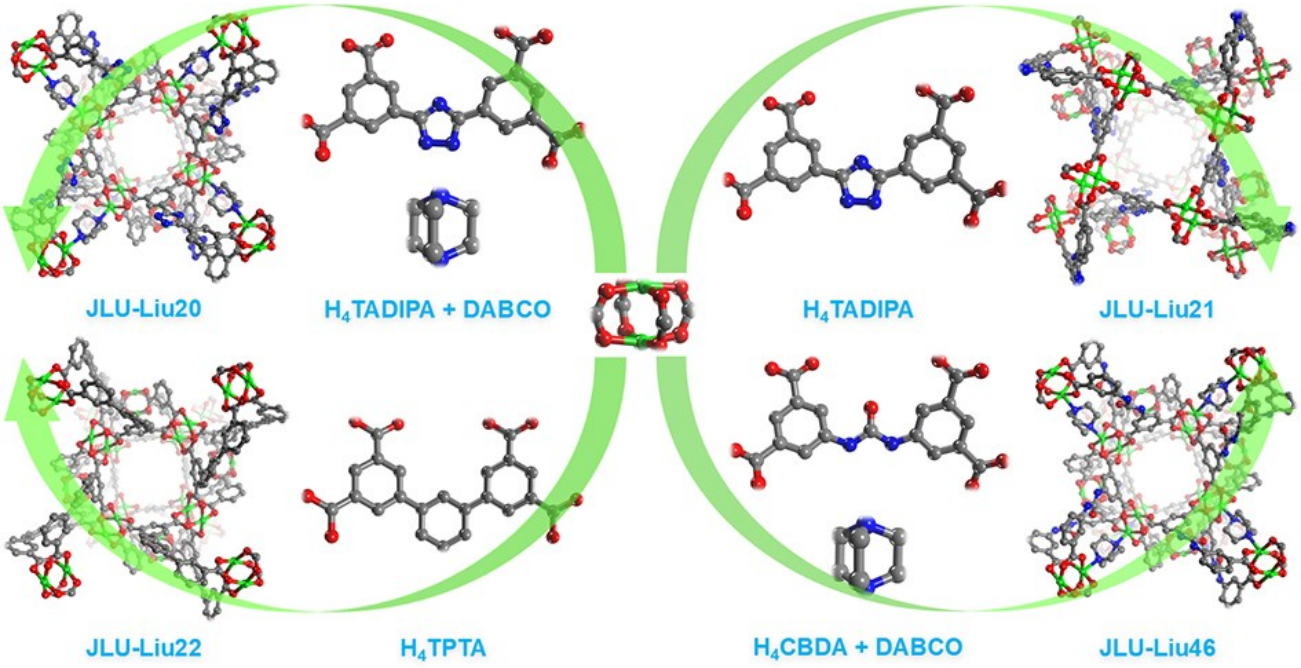

Figure S1. Structure features for the four Cu-PMOFs.

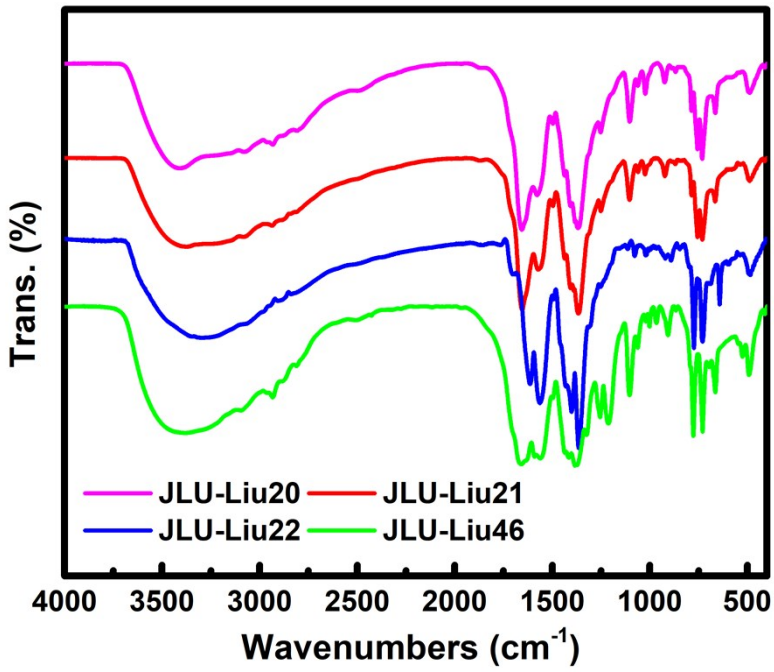

Figure S2. The infrared spectra for four Cu-PMOFs.

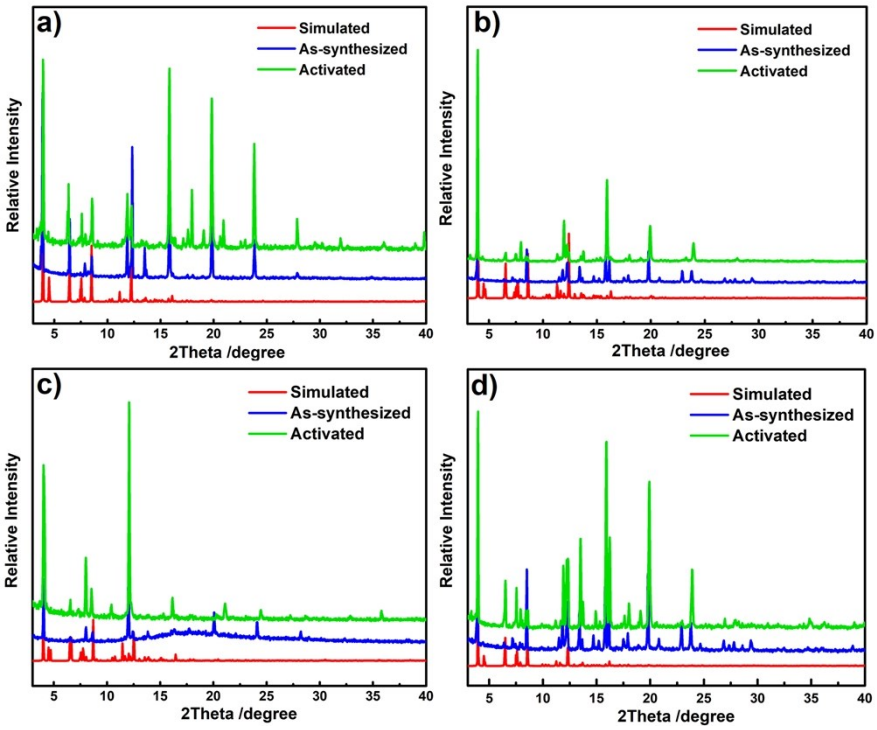

Figure S3. PXRD patterns for (a) **JLU-Liu20**, (b) **JLU-Liu21**, (c) **JLU-Liu22** and (d) **JLU-Liu46**.

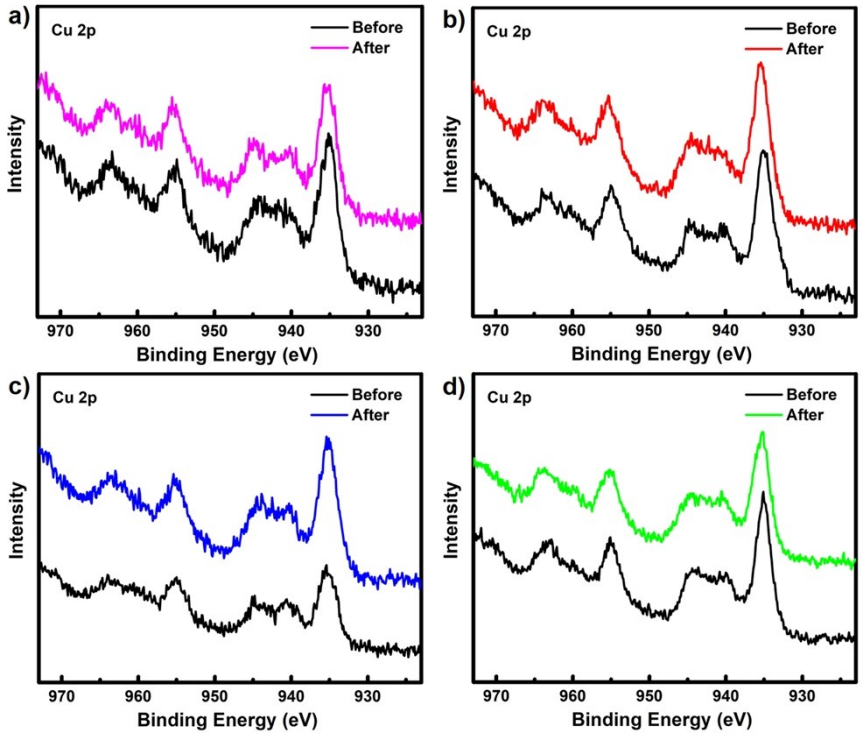

Figure S4. XPS spectra of a) **JLU-Liu20**, b) **JLU-Liu21**, c) **JLU-Liu22** and d) **JLU-Liu46** samples before and after cycloaddition reaction.

A continuous sampling experiment was undertaken at 1, 6, 12, 18, 24, 36 and 48 hours to investigate the influence of reaction time on PC's yield (20 mmol PO, 0.25 mol % Cu-paddlewheel, 5 mol % TBAB and 1 bar CO_2 at 25 ^oC). As shown in **Figure S4**, before 12 hours the curve was almost straight, which showed that the reaction was within the kinetic interval. From 12 to 24 hours, the decline of the curve slope displayed that the inflexion existed in the interval.

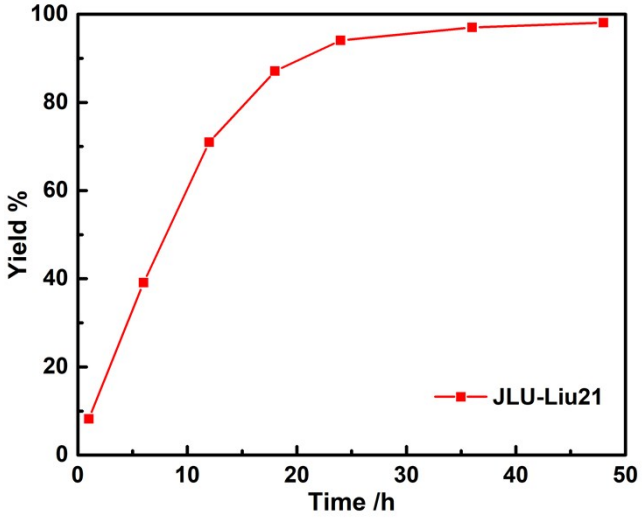

Figure S5. Continuous sampling experiment of **JLU-Liu21** for cycloaddition reaction of PO with CO_2.

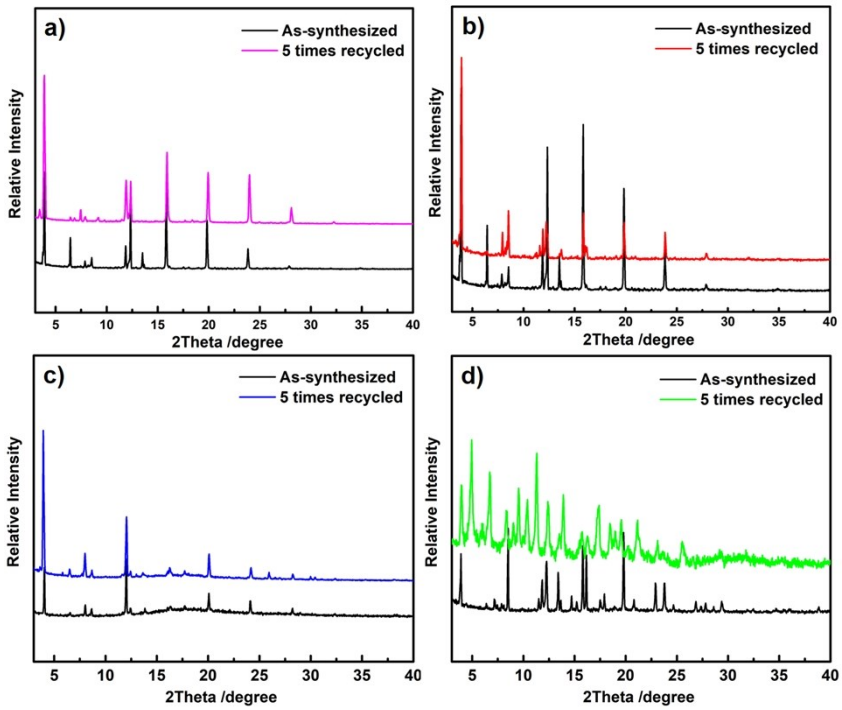

Figure S6. PXRD patterns of a) **JLU-Liu20**, b) **JLU-Liu21**, c) **JLU-Liu22** and d) **JLU-Liu46** for as-synthesized samples and after 5 times recycled samples.

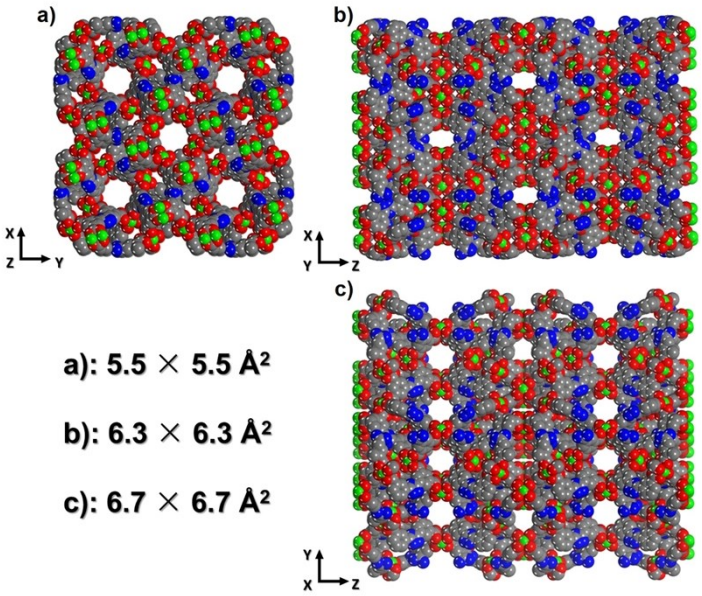

Figure S7. Space-filling view of **JLU-Liu21** with multiple pores in different directions.

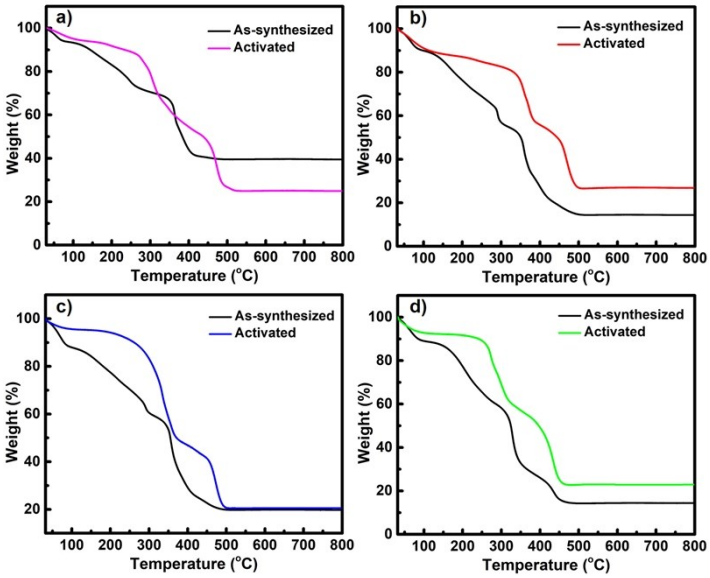

Figure S8. TGA curves for as-synthesized and activated samples of a) **JLU-Liu20**, b) **JLU-Liu21**, c) **JLU-Liu22** and d) **JLU-Liu46**.

S2 Cycloaddition reaction of CO_2 with epoxides

Details of experiments and calculation procedures of catalytic efficiency

In a typical catalytic reaction under 1 bar, epoxide (20 mmol), TBAB (1 mmol, 5 mol %), activated Cu-PMOFs (0.25 mol % for open Cu sites or Cu-paddlewheel based on different reactions, respectively) were put into a 15 mL Schlenk tube with solvent free environment. For high pressure reaction, PO (40 mmol), TBAB (2 mmol), organic ligands (0.1 mmol), $Cu(NO_3)_2{\cdot}3H_2O$ (0.1 mmol) or activated Cu-PMOFs (0.25 mol % open Cu site) were put into a high-pressure reactor. To activate the MOFs materials, the as-synthesized sample were washed by DMF for three times, then put the samples into ethanol for 3 days and change fresh ethanol every 4 h to completely remove the non-volatile solvent molecules. After that, the samples were dried again using the "outgas" function of the surface area analyzer for 10 h at 90 ^oC and collected the MOFs for further cycloaddition reaction.

Before triggering the reaction, pump out the air inside the tube/reactor and fill in with pure CO_2 (or post-combustion flue). After 3 times pump-fill procedure, turn the temperature and pressure to specific conditions (1 bar, 25^o C for PO and 80 ^oC for other epoxides in Schlenk tube; 2 MPa, 60 ^oC in high pressure reactor). The speed of stirring was 400 rpm (the speed could slow a little down for PO in order to reduce the low-boiling-point compound volatilization in continuous stirring under 1 bar). After centrifuging to recycle the catalyst, a little supernatant reaction mixture was taken to get analyzed by ^1H NMR.

The yields of PO, ECH, 1, 2-epoxy-3-phenoxypropane, glycidyl-2-methylphenyl ether and cyclohexene oxide (Ha for epoxides and Ha' for carbonates, respectively) catalyzed by the Cu-PMOFs were calculated according to the following equation.

$$Yield(\%) = \frac{I_{Ha'}}{I_{H_a} + I_{Ha'}} \times 100\ \%$$

The yield of SO to styrene carbonate were determined by calculation of the ^1H NMR integrals of corresponding highlighted protons in styrene oxide (Ha), styrene carbonate (Ha') and phenyl group (Hb-Hf) (from SO, styrene carbonate and other by-products) according to the following equation.

$$Yield\ (\%) = \frac{5 \times I_{H_{a'}}}{I_{H_b - H_f}} \times 100\ \%$$

^{1}H NMR spectra

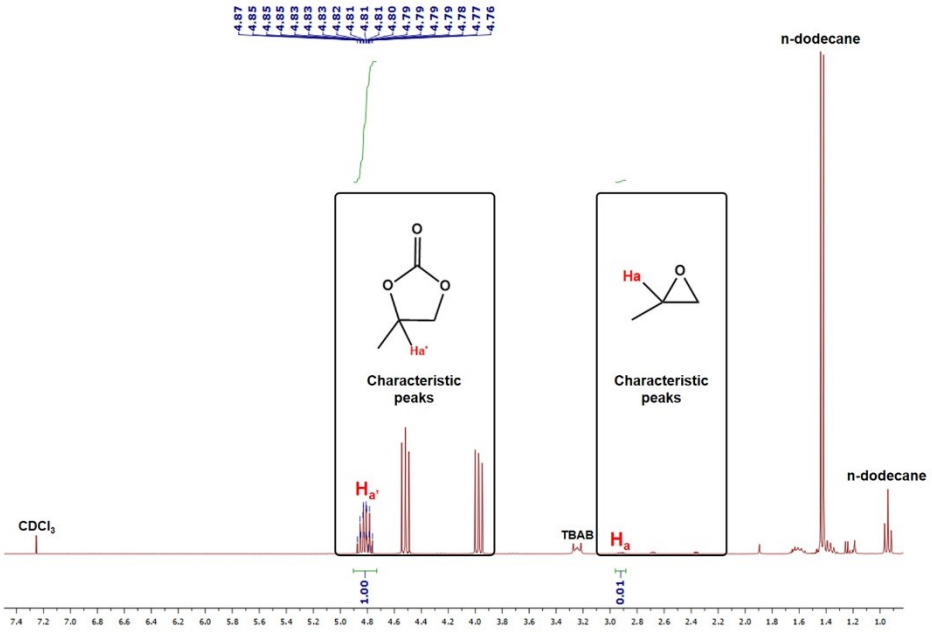

Figure S9. ^{1}H NMR spectrum of the mixture products under pure CO_2 atmosphere catalyzed by **JLU-Liu21** (Table 1, Entry 6) in $CDCl_3$. n-dodecane was used as internal standard.

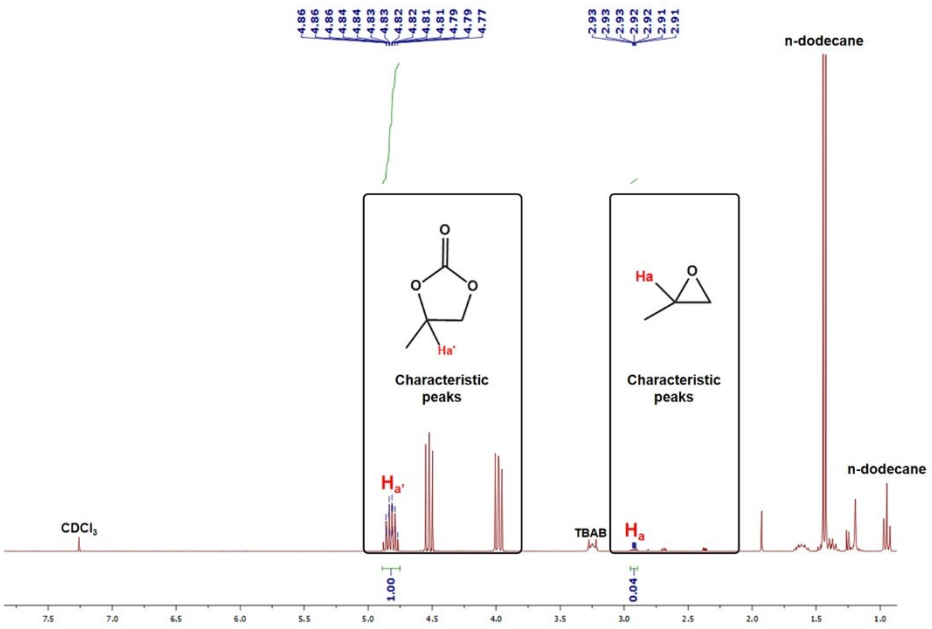

Figure S10. ^{1}H NMR spectrum of the mixture products under pure CO_2 atmosphere catalyzed by **JLU-Liu21** (Table 2, Entry 1) in $CDCl_3$ (n-dodecane was used as internal standard).

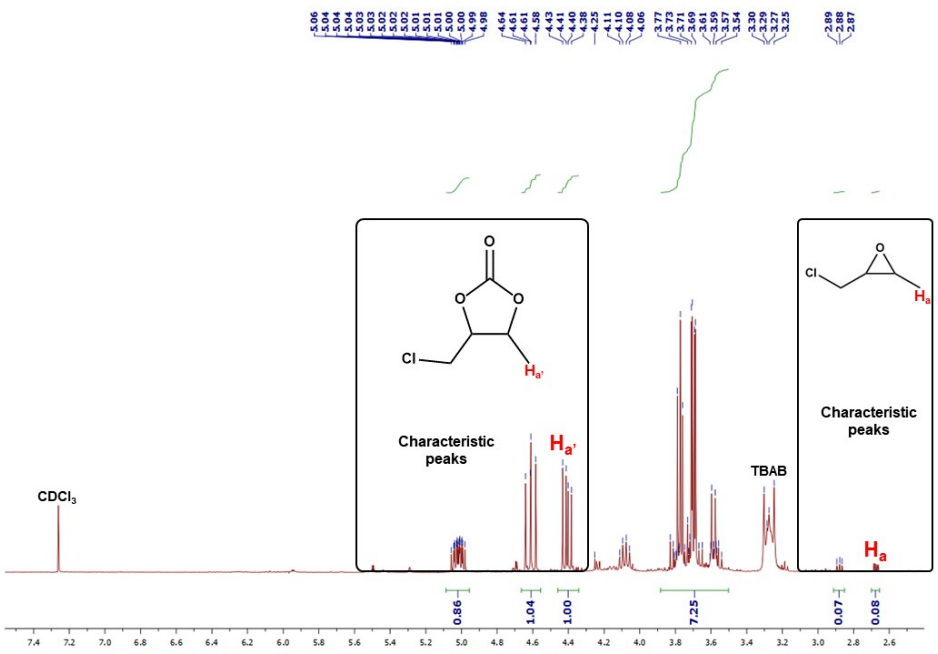

Figure S11. ^{1}H NMR spectrum of the mixture products under pure CO_2 atmosphere catalyzed by **JLU-Liu21** (Table 2, Entry 3) in $CDCl_3$.

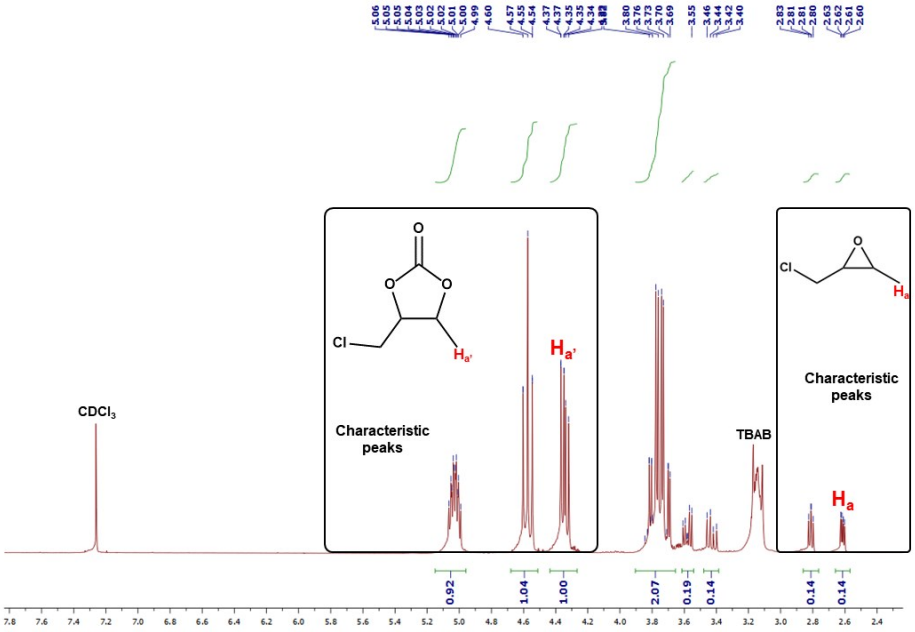

Figure S12. ^{1}H NMR spectrum of the mixture products under pure CO_2 atmosphere catalyzed by **JLU-Liu46** (Table 3, Entry 3) in $CDCl_3$.

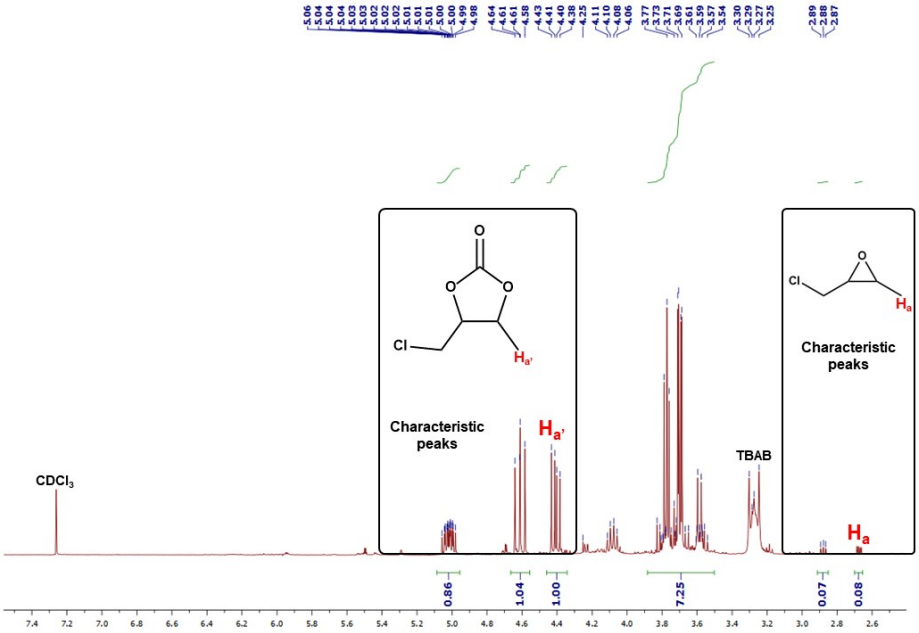

Figure S13. ^{1}H NMR spectrum of the mixture products under pure CO_2 atmosphere catalyzed by **JLU-Liu21** (Table 4, Entry 4) in $CDCl_3$.

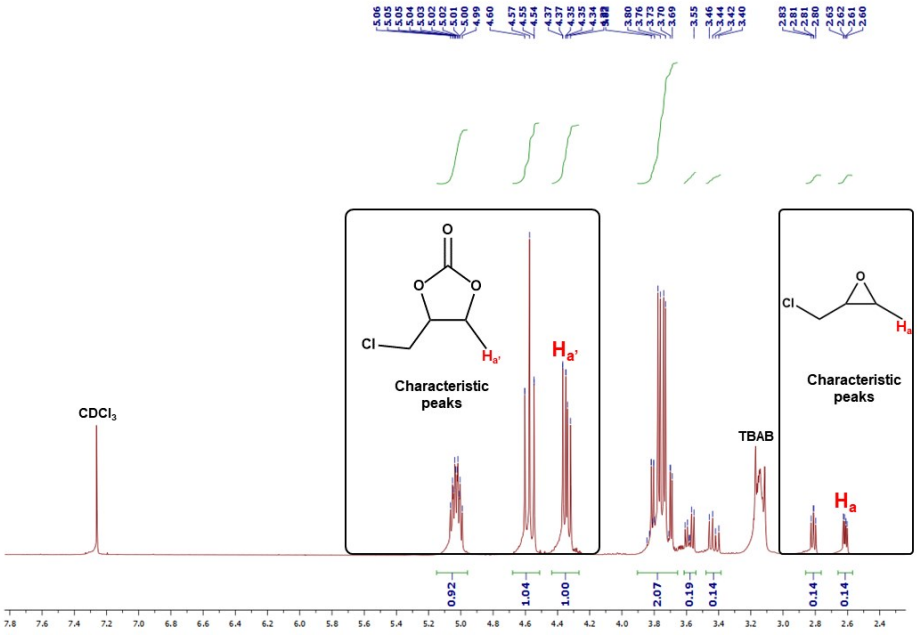

Figure S14. ^{1}H NMR spectrum of the mixture products under post-combustion flue atmosphere catalyzed by **JLU-Liu21** (Table 5, Entry 9) in $CDCl_3$.

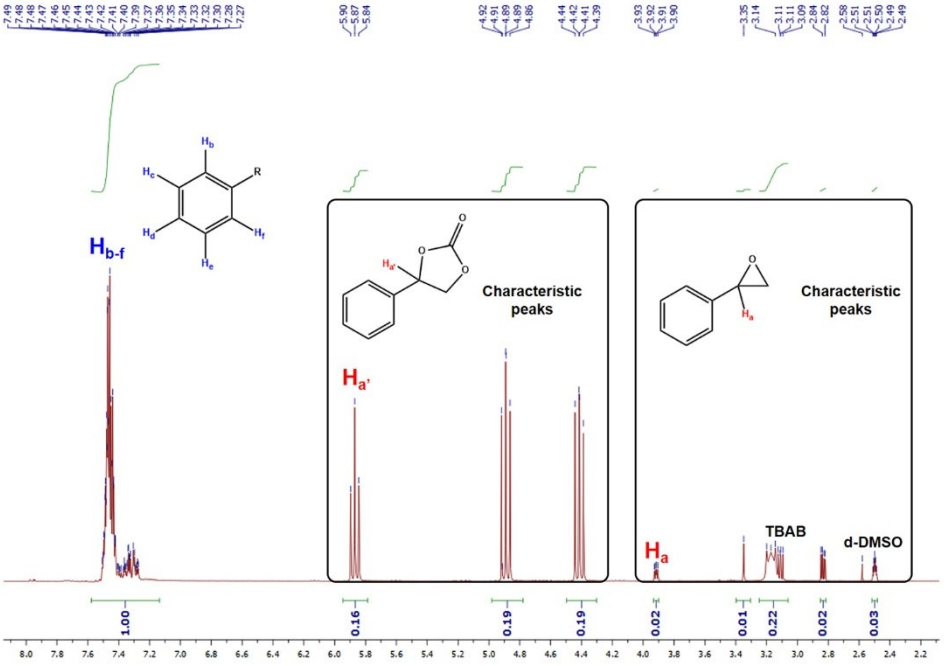

Figure S15. ^{1}H NMR spectrum of the mixture products under post-combustion flue atmosphere catalyzed by **JLU-Liu21** (Table 5, Entry 10) in d-DMSO.

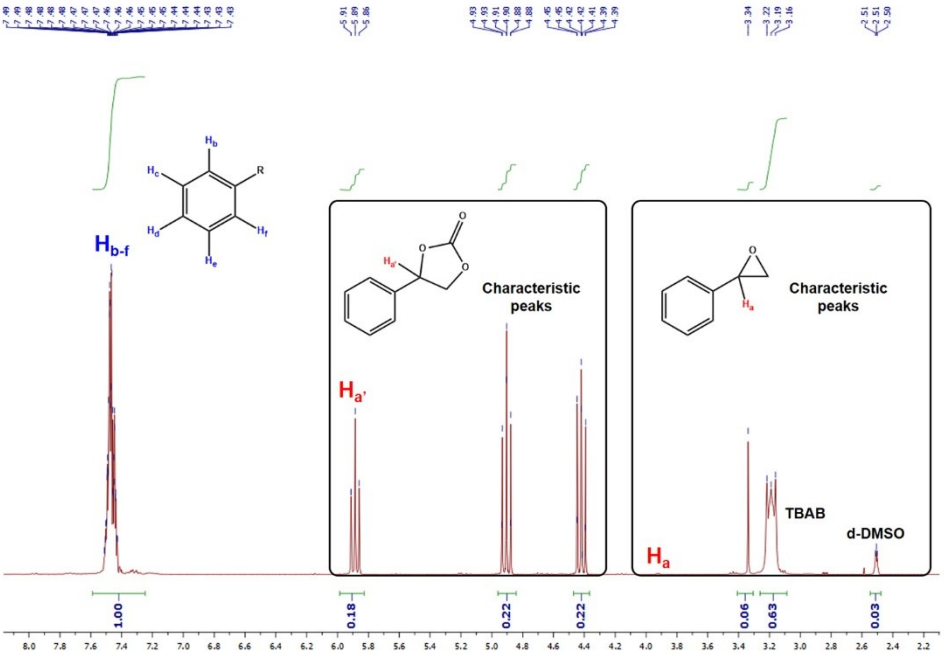

Figure S16. ^{1}H NMR spectrum of the mixture products under pure CO_2 atmosphere catalyzed by **JLU-Liu21** (Table 5, Entry 12) in d-DMSO.

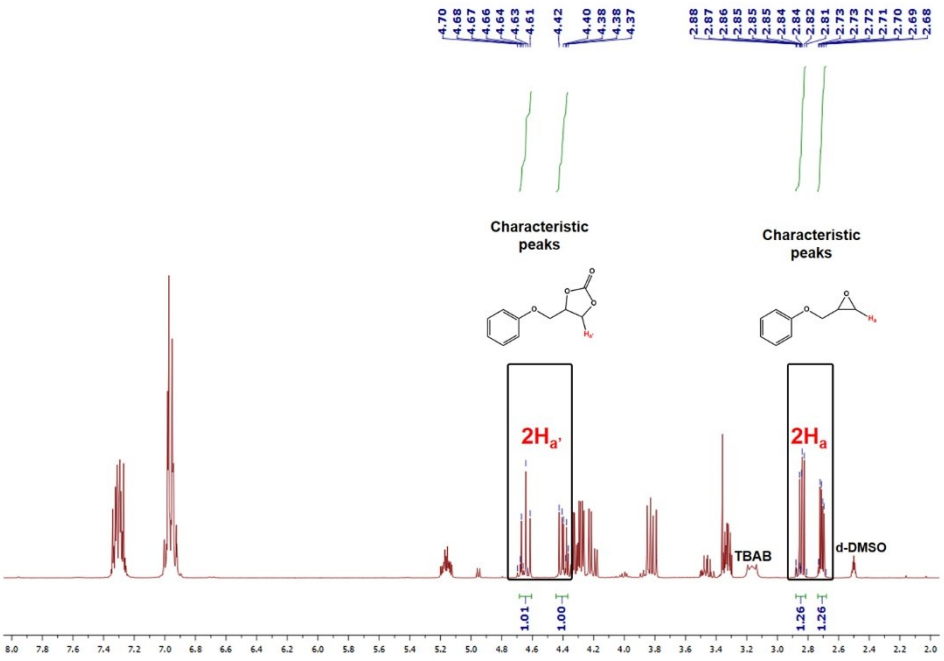

Figure S17. ^{1}H NMR spectrum of the mixture products under pure CO_2 atmosphere catalyzed by **JLU-Liu21** (Table 6, Entry 4) in d-DMSO.

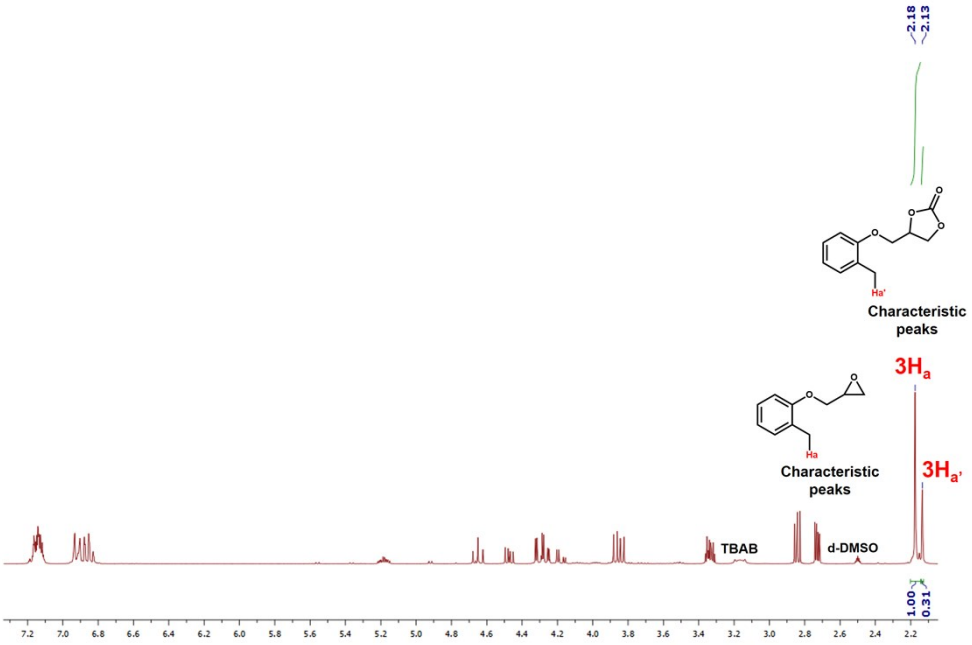

Figure S18. ^{1}H NMR spectrum of the mixture products under pure CO_2 atmosphere catalyzed by **JLU-Liu21** (Table 6, Entry 6) in d-DMSO.

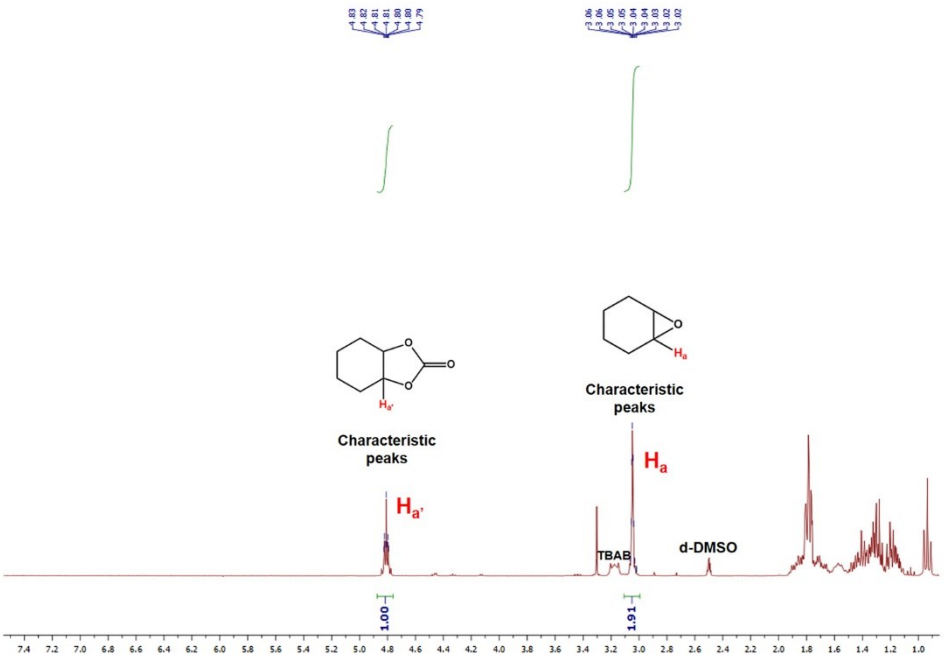

Figure S19. ^{1}H NMR spectrum of the mixture products under pure CO_2 atmosphere catalyzed by **JLU-Liu21** (Table 6, Entry 8) in d-DMSO.

S3. Supporting Tables

Table S1. Empirical formula and number of Cu open sites for the four Cu-PMOFs.

Cu-PMOFs	JLU-Liu20	JLU-Liu21	JLU-Liu22	JLU-Liu46
Empirical formula	$C_{87}H_{126}Cu_6N_{20}O_{48}$	$C_{87}H_{121}Cu_6N_{17}O_{54}$	$C_{111}H_{156}Cu_6N_{11}O_{50}$	$C_{72}H_{91}Cu_6N_{13}O_{42}$
Number of Cu open sites[a]	16	24	24	16

[a] Twelve Cu-paddlewheels exist in each single MOP, four coordinated DABCO molecules in **JLU-Liu20** and **JLU-Liu46** which lead to their fewer open Cu sites than that of **JLU-Liu21** and **JLU-Liu22**.

Table S2. Sizes of some epoxides (van der Waals radii were determined by Bondi).

Epoxides	Size (Å^3)
Propylene oxide	6.1 × 4.4 × 5.0
Epichlorohydrin	7.2 × 5.6 × 5.1
Styrene oxide	9.3 × 6.9 × 4.6
1, 2-epoxy-3-phenoxypropane	12.5 × 7.1 × 5.4
Glycidyl-2-methylphenyl ether	12.6 × 7.8 × 5.2
Cyclohexene oxide	6.5 × 7.0 × 5.0

Table S3. CO_2 uptake for four compounds.

Compounds	CO_2 uptake (cm^3g^{-1})		References
	273 K	298 K	
JLU-Liu20	162	88	25
JLU-Liu21	210	118	25
JLU-Liu22	170	95	27
JLU-Liu46	185	104	26

Table S4. ICP-OES analysis of Cu^{2+} in the 5th cycled reaction mixture filtrate.

Catalysts	JLU-Liu20	JLU-Liu21	JLU-Liu22	JLU-Liu46
Cu^{2+} concentration (ppm)	0.0292	0.0236	0.0304	0.0253

ICP-OES analysis of the fifth product filtrate catalyzed by four Cu-PMOFs catalysts (Table S4), which indicated almost no Cu^{2+} ions leaked after the catalytic experiment.

Table S5. Density of OMSs, LBSs and Q_{st} of CO_2 for four Cu-PMOFs.

Compounds	Density of OMSs (nm^{-3})	Density of LBSs (nm^{-3})	Q_{st} (kJ /mol)	References
JLU-Liu20	1.08	2.3	32	25
JLU-Liu21	1.69	2.39	28	25
JLU-Liu22	1.0	0	30	27
JLU-Liu46	1.11	1.52	32	26

Table S6. Comparisons of some reported MOFs-based catalysts in cycloaddition reaction of CO_2 with PO under relatively high temperature and pressure.

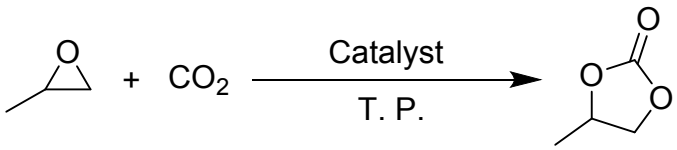

Entry	Catalysts	Tem. (°C)	P (bar)	Time (h)	Yield (%)	Ref.
1	$(Cu_2BPDSDC{\cdot}4DMF){\cdot}2DMF$[a]	80	25	5	99	1
2	IL@ZIF-8(Zn/Co)[b]	100	10	2	99	2
3	**JLU-Liu21**	**60**	**20**	**6**	**99**	**This work**
4	PCN-224[i]	50	4	24	99	17
5	67BPym-MeI[d]	100	5	24	99	13
6	$Zn_3(L)_3(H_2L)$[c]	80	10	5	99	12
7	$[(CH_3)_2NH_2][Zn_{1.5}(\mu_3\text{-}O)_{0.5}$(F-tzba)$_{1.25}(bpy)_{0.25}(\mu_2\text{-}F)_{0.5}]{\cdot}2DMF{\cdot}2H_2O$[e]	80	20	4	98	4
8	RH Au/Zn-MOF[h]	70	30	24	98	16
9	MIL-IMAc-Br[l]	60	5	20	98	19
10	IL-$[In_2(dpa)_3$(1,10-phen)$_2]$[f]	60	12	6	97	5
11	**JLU-Liu20**	**60**	**20**	**6**	**97**	**This work**
12	$ZnC_{20}H_{20}N_4O_5$[g]	80	10	18	97	15
13	NUC-5[j]	80	1	24	97	18
14	**JLU-Liu46**	**60**	**20**	**6**	**96**	**This work**
15	RD Au/Zn-MOF[h]	70	30	24	96	16
16	$CdC_{20}H_{20}N_4O_5$[g]	80	10	18	95	15
17	MIL-101-tzmOH-Br[k]	80	100	10	93	9
18	**JLU-Liu22**	**60**	**20**	**6**	**92**	**This work**
19	MOF-525[i]	50	4	24	85	17
20	PCN-222[i]	50	4	24	66	17

[a] Reaction conditions: PO (12.5 mmol), catalyst (50 mg), TBAB (0.1g), [b] catalyst (100 mg), [c] PO (34.5 mmol), catalyst (0.1 g), TBAB (0.1 g), [d] PO (20 mmol), catalyst (50 mg), [e] catalyst (0.2 mol %), TBAB (2 mol %), [f] catalyst (0.2 mol %), [g] catalyst (42.6 mmol), TBAB (1.8 mol %), [h] catalyst (36 mg, 0.07 mmol Au), [i] catalyst (0.1 mol % metal), TBAB (10 mol%), [j] catalyst (1.5 mol %), TBAB (5 mol %), [k] catalyst (0.17 mol % metal center), [l] PO (30 mmol), catalyst (0.068 mmol).

Table S7. Comparison for cycloaddition reaction of PO with CO_2 to some reported high-level performing MOFs-based catalysts under respectively optimized conditions in pure CO_2 atmosphere.

Entry	Catalysts	Tem. (°C)	P (bar)	Time (h)	Yield (%)	Ref.
1	$(Cu_2BPDSDC{\cdot}4DMF){\cdot}2DMF$[a]	80	25	5	99	1
2	IL@ZIF-8(Zn/Co)[b]	100	10	2	99	2
3	$Cu_5(TPTC)_3(BPDC\text{-}Urea)_{0.5}(H_2O)_5$[c]	25	1	36	98	1
4	**JLU-Liu21**	**25**	**1**	**48**	**98**	**This work**
5	MOF-74-III(Co)-1[d]	25	12	48	98	3
6	$[(CH_3)_2NH_2][Zn_{1.5}(\mu_3\text{-}O)_{0.5}(F\text{-}tzba)_{1.25}(bpy)_{0.25}(\mu_2\text{-}F)_{0.5}]{\cdot}2DMF{\cdot}2H_2O$[e]	80	20	4	98	4
7	IL-$[In_2(dpa)_3(1,10\text{-}phen)_2]$[f]	60	12	6	97	5
8	$Cu_4(L_8)$[g]	25	1	48	96	6
9	JUC-1000[h]	25	1	48	96	7
10	Cu_4MTTP[i]	25	1	48	96	6
11	MMCF-2[j]	25	1	48	95	8
12	MIL-101-tzmOH-Br[k]	80	10	10	93	9
13	**JLU-Liu21 (post-combustion flue)**	**25**	**1**	**48**	**92**	**This work**
14	MMPF-9[j]	25	1	48	87	10
15	MOF-892	25	1	60	70	14
16	HKUST-1[i]	25	1	48	65	6
17	$Cu_5(TPTC)_3(BPDC\text{-}NH_2)_{0.5}(H_2O)_5$[a]	25	1	36	50	1
18	$[(CH_3)_2NH_2][Zn_{1.5}(\mu_3\text{-}O)_{0.5}(F\text{-}tzba)_{1.25}(bpy)_{0.25}(\mu_2\text{-}F)_{0.5}]{\cdot}2DMF{\cdot}2H_2O$[e]	25	1	48	45	4
19	MOF-505[i]	25	1	48	48	8
20	$Cu_5(TPTC)_3(BPDC)_{0.5}(H_2O)_5$[c]	25	1	36	40	1
21	$(Zn_4O)(Zn_3CuO)(Cu_2)_{1.5}(L)_6(H_2O)_3$[c]	25	11.8	60	32	11

[a] Reaction conditions: PO (12.5 mmol), catalyst (50 mg), TBAB (0.1g), [b] catalyst (100 mg), [c] catalyst (0.25 mol % Cu-paddlewheel), [d] catalyst (0.05 mol %), TBAB (3.75 mol %), [e] catalyst (0.2 mol %), TBAB (2 mol %), [f] catalyst (0.2 mol %), [g] catalyst (0.2 mol % per Cu-paddlewheel), TBAB (10 mol %), [h] catalyst (0.016 mol % Cu-paddlewheel), TBAB (3.75 mol %), [i] catalyst (0.2 mol % Cu-paddlewheel), TBAB (10 mol %), [j] catalyst (0.125 mol % Cu-paddlewheel), TBAB (0.58g), [k] catalyst (0.17 mol % metal center) [l] catalyst (0.32 mol %), TBAB(8 mol %).

Table S8. Comparison for cycloaddition reaction of PO, ECH and SO by JLU-Liu21 to other reported MOFs-based catalysts under respectively optimized conditions (20 mmol epoxide, 5 mol % TBAB) in post-combustion flue atmosphere (15 % CO_2 and 85 % N_2).

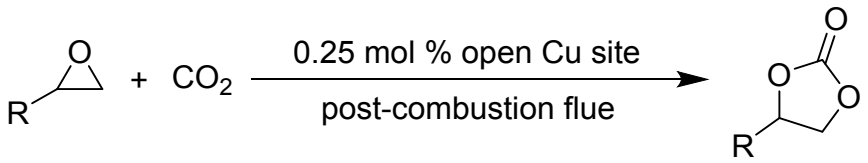

Entry	R	Catalysts	Tem. (°C)	P (bar)	Time (h)	Yield (%)	Ref.
1	CH_3	**JLU-Liu21**	25	1	48	92	**This work**
2	CH_3	I_{C2}HCP-5b[b]	120	30	20	85	21
3	CH_3	Zn(Bmic)(AT)[a]	25	1	48	5	20
4	CH_2Cl	FJI-H14[c]	80	1	24	95	22
5	CH_2Cl	**JLU-Liu21**	80	1	48	88	**This work**
6	CH_2Cl	I_{C2}HCP-5b[b]	120	30	4	81	21
7	CH_2Cl	I_{C2}HCP-5[b]	120	30	4	77	21
8	CH_2Cl	I_{C2}HCP-1[b]	120	30	4	76	21
9	CH_2Cl	I_{C2}HCP-5a[b]	120	30	4	75	21
10	CH_2Cl	I_{C2}HCP-10[b]	120	30	4	73	21
11	CH_2Cl	I_{C2}HCP-5c[b]	120	30	4	72	21
12	CH_2Cl	$[Co_6(TATAB)_4(DABCO)_3(H_2O)_3]\cdot 12DMF\cdot 9H_2O$[d]	80	4	15	63	23
13	Ph	InDCPN-Cl[e]	80	1	48	91	24
14	Ph	I_{C2}HCP-5b[b]	120	30	4	87	21
15	Ph	FJI-H14[c]	80	1	24	86	22
16	Ph	**JLU-Liu21**	80	1	48	80	**This work**
17	Ph	HKUST-1	80	1	24	67	22

[a] Reaction conditions: PO (34.5 mmol), catalyst (0.187 mmol), TBAB (0.50 mmol); [b] Epoxide (50 mmol), catalyst (0.01 mmol ionic sites), no co-catalyst; [c] ECH (20 mmol), catalyst (0.48 mol % per Cu units), TBAB (2.5 mol %); [d] ECH (20 mmol), catalyst (0.2 mol %), CO_2:N_2 = 13:87; [e] Epoxide (20 mmol), catalyst (0.05 mol %), TBAB (5 mol %).

Table S9. Optimum conditions for cycloaddition of CO_2 with PO catalyzed by four Cu-PMOFs.

	Tem. (°C)	Time (h)	Yield (%)	TON[a]	TOF (h^{-1})[b]
0.25 mol % open Cu site 5 % TBAB, 1 bar **JLU-Liu20**	25	1	27	108	108.0
	25	6	46	184	30.1
	25	12	59	236	19.7
	25	18	69	276	15.3
	25	24	76	304	12.7
	25	36	85	340	9.4
	25	48	90	360	7.5
0.25 mol % open Cu site 5 % TBAB, 1 bar **JLU-Liu21**	25	1	32	128	128.0
	25	6	54	216	36.0
	25	12	69	276	23.0
	25	18	79	316	17.6
	25	24	86	344	14.3
	25	36	94	376	10.4
	25	48	98	392	8.2
0.25 mol % open Cu site 5 % TBAB, 1 bar **JLU-Liu22**	25	1	22	88	88.0
	25	6	36	144	24.0
	25	12	49	196	16.3
	25	18	61	244	13.6
	25	24	72	288	12.0
	25	36	81	324	9.0
	25	48	86	344	7.2
0.25 mol % open Cu site 5 % TBAB, 1 bar **JLU-Liu46**	25	1	19	76	76.0
	25	6	32	128	21.3
	25	12	46	184	15.3
	25	18	58	232	12.9
	25	24	70	280	11.7
	25	36	79	316	8.8
	25	48	85	340	7.1

[a] Turnover number (product (mmol)/metal (mmol)); [b] Turnover frequency (product (mmol)/metal(mmol)/time (h)).

Table S10. Optimum conditions for cycloaddition of CO_2 with ECH catalyzed by four Cu-PMOFs.

	Tem. (°C)	Time (h)	Yield (%)	TON[a]	TOF (h^{-1})[b]
0.25 mol % open Cu site 5 % TBAB, 1 bar **JLU-Liu20**	80	1	22	88	88.0
	80	6	39	156	26.0
	80	12	54	216	18.0
	80	18	65	260	14.4
	80	24	72	288	12.0
	80	36	77	308	8.6
	80	48	80	320	6.7
0.25 mol % open Cu site 5 % TBAB, 1 bar **JLU-Liu21**	80	1	21	84	84.0
	80	6	40	160	26.7
	80	12	56	224	18.7
	80	18	70	280	15.6
	80	24	81	324	13.5
	80	36	88	352	9.8
	80	48	92	368	7.7
0.25 mol % open Cu site 5 % TBAB, 1 bar **JLU-Liu22**	80	1	14	56	56.0
	80	6	29	116	19.3
	80	12	43	172	14.3
	80	18	55	220	12.2
	80	24	64	256	10.7
	80	36	70	280	7.8
	80	48	74	296	6.2
0.25 mol % open Cu site 5 % TBAB, 1 bar **JLU-Liu46**	80	1	21	84	84.0
	80	6	36	144	24.0
	80	12	49	196	16.3
	80	18	61	244	13.6
	80	24	68	272	11.3
	80	36	73	292	8.1
	80	48	77	308	6.4

[a] Turnover number (product (mmol)/metal (mmol)); [b] Turnover frequency (product (mmol)/metal(mmol)/time (h)).

Table S11. Optimum conditions for cycloaddition of CO_2 with SO catalyzed by four Cu-PMOFs.

	Tem. (°C)	Time (h)	Yield (%)	TON[a]	TOF (h^{-1})[b]
0.25 mol % open Cu site 5 % TBAB, 1 bar **JLU-Liu20**	80	1	16	64	64.0
	80	6	34	136	22.7
	80	12	49	196	16.3
	80	18	61	244	13.6
	80	24	71	284	11.8
	80	36	77	308	8.6
	80	48	80	320	6.7
0.25 mol % open Cu site 5 % TBAB, 1 bar **JLU-Liu21**	80	1	29	116	116
	80	6	45	180	30.0
	80	12	59	236	19.7
	80	18	71	284	15.8
	80	24	80	320	13.3
	80	36	86	344	9.6
	80	48	90	360	7.5
0.25 mol % open Cu site 5 % TBAB, 1 bar **JLU-Liu22**	80	1	18	72	72.0
	80	6	30	120	20.0
	80	12	40	160	13.3
	80	18	49	196	10.9
	80	24	56	224	9.3
	80	36	61	244	6.8
	80	48	65	260	5.4
0.25 mol % open Cu site 5 % TBAB, 1 bar **JLU-Liu46**	80	1	19	76	76.0
	80	6	30	120	20.0
	80	12	42	168	14.0
	80	18	53	212	11.8
	80	24	60	240	10.0
	80	36	65	260	7.2
	80	48	68	272	5.7

[a] Turnover number (product (mmol)/metal (mmol)); [b] Turnover frequency (product (mmol)/metal(mmol)/time (h).

References

1. L. Wei and B. Ye, Efficient conversion of CO_2 *via* grafting urea group into a $[Cu_2(COO)_4]$-based metal-organic framework with hierarchical porosity, *Inorg. Chem.* 2019, **58**, 4385-4393.
2. Y. Sun, X. Jia, H. Huang, X. Guo, Z. Qiao and C. Zhong, Solvent-free mechanochemical route for the construction of ionic liquid and mixed-metal MOF composites for synergistic CO_2 fixation, *J. Mater. Chem. A* 2020, **8**, 3180-3185.
3. W. Meng, Y. Zeng, Z. Liang, W. Guo, C. Zhi, Y. Wu, R. Zhong, Chong Qu and R. Zou, Tuning expanded pores in metal-organic frameworks for selective capture and catalytic conversion of carbon dioxide, *ChemSusChem* 2018, **11**, 3751-3757.
4. Y. Li, G. Wang, H. Yang, L. Hou, Y. Wang and Z. Zhu, Novel cage-like MOF for gas separation, CO_2 conversion and selective adsorption of an organic dye, *Inorg. Chem. Front.* 2020, **7**, 746-755.
5. R. Babu, J. F. Kurisingal, J. Chang and D. Park, Bifunctional pyridinium-based ionic-liquid-immobilized diindium tris(diphenic acid) bis(1,10-phenanthroline) for CO_2 fixation, *ChemSusChem* 2018, **11**, 924-932.
6. P. Li, X. Wang, J. Liu, J. Lim, R. Zou and Y. Zhao, A triazole-containing metal-organic framework as a highly effective and substrate size-dependent catalyst for CO_2 conversion, *J. Am. Chem. Soc*. 2016, **138**, 2142-2145.
7. H. He, Q. Sun, W. Gao, J. A. Perman, F. Sun, G. Zhu, B. Aguila, K. Forrest, B. Space and S. Ma, A stable metal-organic framework featuring a local buffer environment for carbon dioxide fixation, *Angew. Chem. Int. Ed*. 2018, **57**, 4657-4662.
8. W. Gao, Y. Chen, Y. Niu, K. Williams, L. Cash, P. J. Perez, L. Wojtas, J. Cai. Y. Chen and S. Ma, Crystal engineering of an nbo topology metal-organic framework for chemical fixation of CO_2 under ambient conditions, *Angew. Chem. Int. Ed*. 2014, **53**, 2615-2619.
9. L. Zhou, W. Sun, N. Yang, P. Li, T. Gong, W. Sun, Q. Sui and E. Gao, A facile and versatile “click” approach toward multifunctional ionic metal-organic frameworks for efficient conversion of CO_2, *ChemSusChem* 2019, **12**, 2202-2210.
10. W. Gao, L. Wojtas and S. Ma, A porous metal-metalloporphyrin framework featuring high-density active sites for chemical fixation of CO_2 under ambient conditions, *Chem. Commun*. 2014, **50**, 5316-5318.
11. R. Zou, P. Li, Y. Zeng, J. Liu, R. Zhao, H. Duan, Z. Luo, J. Wang, R. Zou and Y. Zhao, Bimetallic metal-organic frameworks: probing the Lewis acid site for CO_2 conversion, *Small* 2016, **12**, 2334-2343.

12. Z. Gao, X. Zhang, P. Xu and J. Sun, Dual hydrogen-bond donor group-containing Zn-MOF for the highly effective coupling of CO_2 and epoxides under mild and solvent-free conditions, *Inorg. Chem. Front*. 2020, **7**, 1995-2005.
13. H. Ji, K. Naveen, W. Lee, T. Kim, D. Kim and D. Cho, Pyridinium-functionalized ionic metal-organic frameworks designed as bifunctional catalysts for CO_2 fixation into cyclic carbonates, *ACS Appl. Mater. Interfaces* 2020, **12**, 24868-24876.
14. P. T. K. Nguyen, H. T. D. Nguyen, H. N. Nguyen, C. A. Trickett, Q. T. Ton, E. Gutiérrez-Puebla, M. A. Monge, K. E. Cordova and F. Gándara, New metal-organic frameworks for chemical fixation of CO_2, *ACS Appl. Mater. Interfaces* 2018, **10**, 733-744.
15. B. Parmer, P. Patel, R. I. Kureshy, N. H. Khan and E. Suresh, Sustainable heterogeneous catalysts for CO_2 utilization by using dual ligand Zn^{II}/Cd^{II} metal-organic frameworks, *Chem. Eur. J.* 2018, **24**, 15831-15839.
16. L. Tang, S. Zhang, Q. Wu, X. Wang, H. Wu and Z. Jiang, Heterobimetallic metal-organic framework nanocages as highly efficient catalysts for CO_2 conversion under mild conditions, *J. Mater. Chem. A* 2018, **6**, 2964-2973.
17. K. Epp, A. L. Semrau, M. Cokoja and R. A. Fischer, Dual site Lewis-acid metal-organic framework catalysts for CO_2 fixation: counteracting effects of node connectivity, defects and linker metalation, *ChemCatChem* 2018, **10**, 3506-3512.
18. H. Chen, L. Fan, X. Zhang and L. Ma, Nanocage-based $In^{III}\{Tb^{III}\}_2$-organic framework featuring lotus-shaped channels for highly efficient CO_2 fixation and I_2 capture, *ACS Appl. Mater. Interfaces* 2020, **12**, 27803-27811.
19. D. Ma, Y. Zhang, S. Jiao, J. Li, K. Liu and Z. Shi, A tri-functional metal-organic framework heterogeneous catalyst for efficient conversion of CO_2 under mild and co-catalyst free conditions, *Chem. Commun*. 2019, **55**, 14347-14350.
20. Y. Li, X. Zhang, J. Lan, P. Xu and J. Sun, Porous Zn(Bmic)(AT) MOF with abundant amino groups and open metal sites for efficient capture and transformation of CO_2, *Inorg. Chem*. 2019, **58**, 13917-13926.
21. W. Zhang, F. Ma, L. Ma, Y. Zhou and J. Wang, Imidazolium-functionalized ionic hypercrosslinked porous polymers for efficient synthesis of cyclic carbonates from simulated flue gas, *ChemSusChem* 2020, **13**, 341-350.
22. L. Liang, C. Liu, F. Jiang, Q. Chen, L. Zhang, H. Xue, H. Jiang, J. Qian, D. Yuan and M. Hong, Carbon dioxide capture and conversion by an acid-base resistant metal-organic framework, *Nat. Commun*. 2017, **8**, 1233.
23. B. Ugale, S. Kumar, T. J. D. Kumar and C. M. Nagaraja, Environmentally friendly, co-catalyst-free chemical fixation of CO_2 at mild conditions using dual-walled nitrogen-rich three-dimensional porous metal-organic frameworks, *Inorg. Chem*. 2019, **58**, 3925-3936.

24. Y. Yuan, J. Li, X. Sun, G. Li, Y. Liu, G. Verma and S. Ma, Indium-organic frameworks based on dual secondary building units featuring halogen-decorated channels for highly effective CO_2 fixation, *Chem. Mater*. 2019, **31**, 1084-1091.
25. B. Liu, S. Yao, C. Shi, G. Li, Q. Huo and Y. Liu, Significant enhancement of gas uptake capacity and selectivity *via* the judicious increase of open metal sites and Lewis basic sites within two polyhedron-based metal-organic frameworks, *Chem. Commun*. 2016, **52**, 3223-3226.
26. B. Liu, S. Yao, X. Liu, X. Li, R. Krishna, G. Li, Q. Huo and Y. Liu, Two analogous polyhedron-based MOFs with high density of Lewis basic sites and open metal sites: significant CO_2 capture and gas selectivity performance, *ACS Appl. Mater. Interfaces* 2017, **9**, 32820-32828.
27. D. Wang, B. Liu, S. Yao, T. Wang, G. Li, Q. Huo and Y. Liu, A polyhedral metal-organic framework based on the supermolecular building block strategy exhibiting high performance for carbon dioxide capture and separation of light hydrocarbons, *Chem. Commun.* 2015, **51**, 15287-15289.